tance curves for $U_d = 0$ and $U_d/D = 1$ at $t/D = 0.0001$, where $\Gamma_a/T_K^0 = 1.7 \times 10^{-3}$ since the Kondo temperature (Wilson's definition) is $T_K^0 = 9.7 \times 10^{-5} D$. In this regime the Kondo effect on the embedded dot in no way affects the Fano interference process in the relevant range of energies and temperatures (i.e. several times Γ_a). Only for very large ϵ_a and very high temperature (of the order of T_K^0) will the differences become apparent, however this is outside the parameter regime of interest here.

When Γ_a is equal to a considerable fraction of T_K^0, we start to see small quantitative departure from the Fano line shape already for ϵ_a and T of the order of Γ_a, see Fig. 4, middle panel. This is clearly a consequence of the competition between correlation and interference effects, combined with further thermal effects. As expected, the discrepancy grows with increasing ϵ_a and T.

Finally, for $\Gamma_a \gg T_K^0$, the embedded dot is strongly perturbed by the coupling to the side-dot and the differences become drastic: at finite T, the line-shape differs qualitatively from the Fano form and, in particular, we observe the emergence of non-uniform E-dependence with broad humps around $E \sim \Gamma_a$.

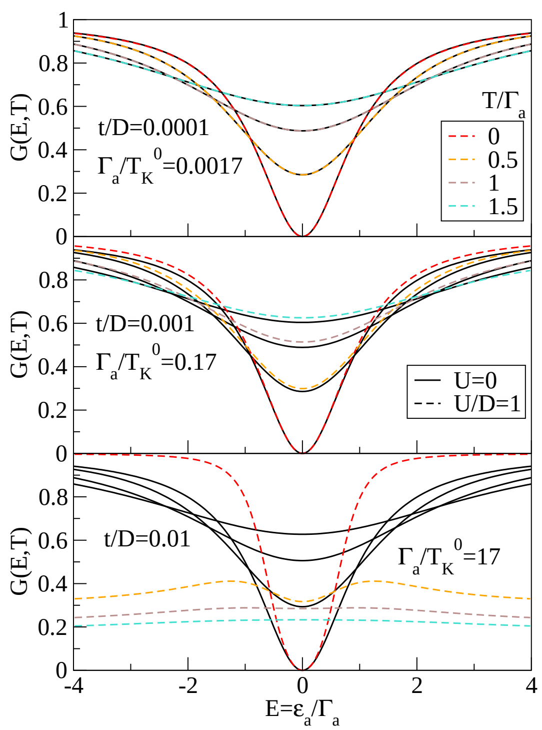

Figure 4: (Color online) Resonance curves for non-interacting (full lines) and interacting models (dashed lines) for a range of scaled temperatures T/Γ_a and for different Γ_a/T_K^0 ratios.

It is instructive to perform curve fitting on the results where the Fano resonance is already strongly perturbed, as shown in Fig. 5. The fits (shown using dashed lines), performed in the energy interval $[-4\Gamma_a : +4\Gamma_a]$, are clearly inadequate. Extracted Fano parameters indicate that the resonance width is significantly reduced below Γ_a and its width even decreases with increasing temperature, which reflects the situation where the spectral function of the embedded dot has a significant variation on the energy scale of Γ_a, which affects the resonance line-shape for large E. It should also be noted that parameters a and b have "unphysical" values $a > 1$ and $b < 0$ for small T. If the curve fitting is performed in a narrower energy interval $[-\Gamma_a : +\Gamma_a]$, the asymptotic small-E form of the resonance can be well captured, however the extracted Fano parameters are factitious and therefore of little use. This demonstrates that in the presence of strong competition between the Fano interference and Kondo effect, the curve fitting using the Fano line-shape is not recommended since the results depend very strongly on the energy window where fitting is performed and it is thus not advisable to make any inference based on them.

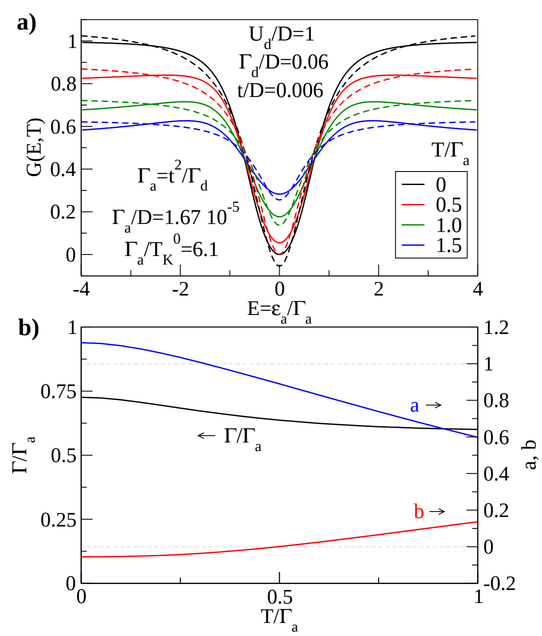

Figure 5: (Color online) Interacting model with $U_d \neq 0$ and $U_a = 0$. Symmetric case, $\epsilon_d = 0$. a) Conductance curves for a range of temperatures. b) Fano parameters as a function of the temperature. Curve fitting is performed in the energy window which corresponds to the horizontal axis in the upper subfigure.

Since there are two different energy scales in the problem (T_K^0 and Γ_a), the temperature-dependence of the conductance is expected to be non-monotonic, as shown in Fig. 6 where we plot the conductance at the bottom of the Fano anti-resonance (i.e. for $\epsilon_a = 0$). Such dependence is a consequence of the competition between the Kondo and Fano effects. The Kondo effect tends to increase the conductance through the formation of many-particle resonance at the Fermi level which opens a new conduction channel through the system. On the other hand, the Fano effect suppresses the conductance through quantum interference. For $T_K^0 \gg \Gamma_a$, the conductance first increases at the higher temperature scale of T_K^0 (the temperature dependence being given by the universal Kondo conductance curve[71]), then it decreases at the lower temperature scale set by Γ_a: see results for $t/D = 0.0001$ and $t/D = 0.001$ in Fig. 6. Note that the unitary limit of full conductance quantum